Melvin M. Evers [1,#]
Menno H. Schut [1,#]
Barry A. Pepers [1]
Melek Atalar [2]
Martine van Belzen [3]
Richard L. Faull [4]
Raymund A.C. Roos [5]
Willeke M.C. van Roon-Mom [1]

[#] Contributed equally to this work

[1] Department of Human Genetics, Leiden University Medical Center
[2] Galapagos B.V., Leiden
[3] Department of Clinical Genetics, Leiden University Medical Center
[4] Centre for Brain Research and Department of Anatomy with Radiology, University of Auckland, New Zealand
[5] Department of Neurology, Leiden University Medical Center

2

Making (anti-) sense out of huntingtin levels in Huntington disease

Neurobiology of Disease 2014, under review

2.1. Abstract

Huntington disease (HD) is an autosomal dominant neurodegenerative disorder, characterized by motor, psychiatric and cognitive symptoms. HD is caused by a CAG repeat expansion in the first exon of the *HTT* gene, resulting in an expanded polyglutamine tract at the N-terminus of the huntingtin protein. Typical disease onset is around mid-life (adult-onset HD) whereas onset below 21 years is classified as juvenile HD. While much research has been done on the underlying HD disease mechanisms, little is known about regulation and expression levels of huntingtin RNA and protein.

In this study we used a unique collection of human *post-mortem* HD brain tissue and fibroblast cells to investigate huntingtin mRNA and protein expression, as well as huntingtin antisense isoforms. In adult-onset HD brain samples, there was only a small but significant lower expression of mutant huntingtin mRNA compared to wild-type huntingtin mRNA, while protein expression levels were equal. Juvenile HD subjects did show a lower protein expression of mutant huntingtin compared to wild-type huntingtin protein. Additionally, in brain tissue we did not find any evidence for a reduced expression of huntingtin antisense with an expanded CTG repeat, as we showed HTTAS_v1 expression in a homozygous HD patient. Finally, we have identified a novel huntingtin antisense isoform and named it HTTAS_v2.2.

Our results highlight subtle differences in huntingtin RNA and protein expression with less mutant huntingtin mRNA, but equal wild-type and mutant huntingtin protein levels in adult-onset HD. In juvenile HD mutant huntingtin protein levels were lower compared with wild-type huntingtin. This indicates subtle differences in huntingtin protein expression between adult-onset and juvenile HD.

2.2. Introduction

Huntington disease (HD) is an autosomal dominant neurodegenerative disorder, characterized by motor, psychiatric and cognitive symptoms (Roos, 2010). HD is caused by a CAG repeat expansion in the first exon of the *HTT* gene on chromosome 4p16, resulting in an expanded polyglutamine (polyQ) tract at the N-terminus of the huntingtin (htt) protein. Carriers of 40 or more CAG repeats will develop HD, whereas people with 36 to 39 repeats show reduced penetrance (Kremer *et al.*, 1992; Losekoot *et al.*, 2013). The mean disease onset lies between 30 and 50 years of age (adult-onset HD). HD patients with onset below 21 years of age (juvenile HD), typically carry more than 55 polyQs (Roos, 2010). The major neuropathology in HD occurs in the striatum and cerebral cortex but degeneration is seen throughout the brain as the disease progresses (Vonsattel and Difiglia, 1998) and insoluble protein aggregates in the nucleus and cytoplasm of cells are a hallmark of the disease (Difiglia *et al.*, 1997).

Knowledge on regulation of htt RNA and protein expression is limited and inconsistent. Upregulation of mutant HTT mRNA translation in HD was suggested by interaction of the expanded CAG repeat with the MID1-PP2A complex (Krauss *et al.*, 2013). Upregulation of mutant HTT mRNA translation was also suggested by HTT antisense transcript regulation (Chung *et al.*, 2011). Two natural HTT antisense transcripts (HTTAS_v1 and v2) were identified at the HTT locus, of which HTTAS_v1 contains a CTG repeat. Overexpression of HTTAS_v1 resulted in reduced HTT transcript levels, whereas HTTAS_v1 knockdown increased HTT transcript levels (Chung *et al.*, 2011). Furthermore, in *post-mortem* HD brain no HTTAS_v1 with expanded CTG repeat could be detected. From these observations, it was suggested that HTTAS_v1 negatively regulated HTT transcript expression (Chung *et al.*, 2011). Contrasting, in patient-derived lymphoblasts, no CAG repeat-related effect on total HTT mRNA was observed (Lee *et al.*, 2013), suggesting that there is no difference in wild-type and mutant HTT RNA expression. To our knowledge, levels of wild-type and mutant htt RNA and protein in human HD tissue have not been assessed systematically.

In this study we have investigated htt mRNA and protein levels in a unique collection of human *post-mortem* HD brain tissue and fibroblasts. For *post-mortem* adult-onset HD brain tissue we detected a small, but significant, decrease in mutant HTT mRNA levels compared to wild-type HTT mRNA. Moreover, both brain tissue and fibroblasts from adult-onset HD patients did not show difference in wild-type and mutant htt protein expression levels. In contrast, juvenile HD fibroblasts and brain tissue showed a small, but significant, lower level of mutant htt protein compared to wild-type htt protein. Furthermore, similar HTTAS levels in (homozygous) HD and controls were found. Additionally, we identified a novel HTTAS isoform and named it HTTAS_v2.2.

2.3. Materials & Methods

Patient-derived fibroblasts and human brain samples

Fibroblasts derived from HD patients and controls were purchased from Coriell Cell Repositories, Camden, USA (**Table 1**). Fibroblasts were cultured at 37°C and 5% CO2 in Minimal Essential Medium (Gibco Invitrogen, Carlsbad, USA) with 15% heat inactivated fetal bovine serum (Clontech, Palo Alto USA), 1% Glutamax (Gibco) and 100 U/ml penicillin/streptomycin (Gibco).

Post-mortem human brain tissue was obtained from the Neurological Foundation of New Zealand Human Brain Bank in the Centre for Brain Research, University of Auckland, and the brain bank from the department of Neurology, Leiden University Medical Center. Tissue was obtained with the families full consent and with the ethical approval of the various institutional Ethics Committees. For a complete list of samples and corresponding clinical information, see **Table 2**.

Table 1. Patient-derived fibroblasts.

Name	CAG 1	CAG 2	Type	Age at Sampling	Age of Onset	Sex
GM02173	44	17	HD	52	NA	F
GM04022	44	18	HD	28	NA	F
GM04855	48	20	HD	11	26	M
GM04857	50	40	homozygous HD	23	28	F
GM04281	71	17	juvenile HD	20	14	F
GM05539	97	22	juvenile HD	10	2	M
GM09197	179	18	juvenile HD	6	NA	M
GM04204	18	17	control	81	NA	M

Samples ranked on CAG repeat size of the longest allele.
M: male, F: female, NA: not assessed.

CAG repeat sizing

Genomic DNA samples were isolated from patient-derived fibroblasts and human brain using the Wizard Genomic DNA Purification Kit (Promega) according to manufacturer's instructions and diluted to 50 µg/ml. The number of CAG repeats in the *HTT* gene was determined by PCR using primers "HD-1" and "HD-3" as described previously (Warner *et al.*, 1993), followed by fragment analysis on an ABI 3130 Automated Capillary DNA Sequencer (Applied Biosystems, Life Technologies Corporation, Carlsbad, USA). The exact PCR conditions are available on request. The 3' CAA and following CAG are not counted. For the polyQ repeat the CAA and CAG triplet are counted and the polyQ repeat is therefore 2 units longer than the CAG repeat size.

RNA and genomic DNA analysis

Post-mortem brain tissue was homogenized using ceramic MagNA Lyser beads (Roche, Mannheim, Germany) by grinding in a Bullet Blender (Next Advance, Averill Park, USA) according

Table 2. *Post-mortem* human brain tissue.

Name	CAG 1	CAG 2	Tissue	PMD	Grade	Age of Death	Age of Onset	Sex
HC103	40	19	MTG	11	1	41	35	M
HC105	42	15	MTG	9	1	67	47	F
HD166	42	17	FC	32	2	80	> 70	M
HC102	43	17	MTG	10	3	64	40	M
HC107	43	19	MTG	3	3	75	58	M
HD193	44	9	FC	18	3	68	44	M
HD188	44	16	FC	NA	3	64	44	M
HD195	44	22	FC	8.5	3	61	NA	F
HD159	47	17	FC	42	3	41	26	F
HC114	47	21	MTG	12	NA	53	30	F
HD192	52	18	FC	62	4	37	NA	M
HC104	53	18	MTG	15	3	40	15	M
HD86	84	17	FC/STR	20	3	20	16	F
HD29	84	20	FC	11	NA	11	8	F
H121	23	18	MTG	6	control	64	control	F

Samples ranked on CAG repeat size of the longest allele. MTG: middle temporal gyrus, FC: frontal cortex, STR: striatum, PMD: post-mortem delay (hours), Grade: neuropathological classification, M: male, F: female, NA: not assessed.

to manufacturer's instructions.

Total RNA was isolated from fibroblast cells and brain tissue using the Aurum Total RNA Mini Kit (BioRad, Hercules, USA), with an on-column DNase treatment for 30 min. RNA was eluted in 40 µl elution buffer and cDNA was synthesized from 1 µg total RNA using the Transcriptor First Strand cDNA Synthesis Kit with oligo (dT) primers at 55°C for 90 min (Roche).

PCR was performed using 1 µl cDNA or genomic DNA, 10x Expand High Fidelity buffer with 15 mM $MgCl_2$ (Roche), 200 µM dNTPs (Roche), 1 M Betaine (Sigma-Aldrich, St. Louis, USA), 15 pmol of both forward primer HttCAGFw: 5'- ATG GCG ACC CTG GAA AAG CTG AT -3' and reverse primer HttCAGRev: 5'- TGA GGC AGC AGC GGC TG -3' (Eurogentec, Liege, Belgium), 3 U Expand High Fidelity enzyme mix (Roche), and PCR grade water to a final volume of 30 µl. The PCR program started with a 2 min initial denaturation at 94°C, followed by 35 cycles of 15 sec denaturation at 94°C, 30 sec annealing at 60°C, 1 min elongation at 72°C, after which a final elongation step was performed at 72°C for 7 min.

PCR products were loaded on a 2% agarose gel diluted in Tris/Borate/EDTA buffer (TBE). DNA gel electrophoresis was performed for 1 hour at 100 V. Intensities of DNA bands were quantified using ImageJ software. Intensity of the HTT mRNA band was divided by the corresponding genomic DNA band to normalize for differences in PCR efficiency between wild-type and mutant HTT due to CAG repeat length.

SNP genotyping and SNP linkage by circularization (SLiC)

The procedure for SNPs rs362273 genotyping and SNP linkage by circularization on human brain tissue was adapted from Liu *et al.* (Liu *et al.*, 2008). One µg of DNase-treated total RNA, together with oligo (dT) primers, was used for cDNA synthesis using SuperScript III First-Strand Synthesis System (Invitrogen). To improve reverse transcription of long cDNA templates, 2 M Betaine and 0.6 M Trehalose (both Sigma-Aldrich) were added to the reaction mixture (Spiess

and Ivell, 2002). cDNA synthesis was performed at 42°C for 2.5 hours, followed by RNase H treatment at 37°C for 20 min. Next, 5 µl cDNA was used as template for long-range PCR and SLiC.

Taqman SNP assay

Quantitative PCR was performed using the LightCycler 480 II (Roche), according to manufacturer's instructions, using a mixture containing 45 ng cDNA, 1xTaqMan® Universal PCR Master Mix, no AmpErase®UNG (Applied Biosystems), 1xTaqMan® SNP Genotyping Assay (Applied Biosystems), and nuclease-free water (Ambion) in a 20µl reaction volume. ACTB (Applied Biosystems, cat#Hs99999903_m1) was included as reference gene. A standard curve was generated using pooled equal amounts of cDNA from all samples. Quantification of the dual-color hydrolysis of both allele-specific fluorescent reporter dyes, FAM ("G" allele) and VIC ("A" allele), was performed with the LightCycler® 480 SW 1.5.1 software using the 2nd derivative method, according to manufacturer's instructions.

HTT antisense determination

RNA isolation as described above. PCR was performed using 1.5 µl cDNA, 10x PCR buffer with 20 mM $MgCl_2$ (Roche), 200 µM dNTPs (Roche), 6 pmol primer, for HTTAS_v1, forward: 5'-CAC CGG GGC AAT GAA TGG-3', reverse: 5'- GTG CGG ATG GCA AGG ACA G -3'; and for HTTAS_v2.1/2.2, forward: 5'-GAA GGC GCG GGG CTC AAC-3', reverse: 5'- TGC AGT GCG GAT GGC AAG GA -3', 2 U FastStart Taq DNA Polymerase (Roche), 1 M ethylene glycol (Sigma-Aldrich, St. Louis, USA), and PCR grade water to a final volume of 30 µl. The PCR program started with a 3 min initial denaturation at 95°C, followed by 40 cycles of 10 sec denaturation at 95°C, 10 sec annealing at 60°C, 10 sec elongation at 72°C, after which a final elongation step was performed at 72°C for 7 min.

PCR products were loaded on a 3% TBE agarose gel and bands were extracted using the NucleoSpin Gel & PCR Clean-up kit (Machery Nagel, Düren, Germany). To identify the sequence of the novel HTTAS isoform, PCR products were cloned into a pGEM-T Easy vector (Promega) and analyzed by Sanger sequencing using a T7-specific forward primer.

Protein isolation

Fibroblasts were detached from the culture surface with a 0.5% Trypsin/EDTA solution. After washing twice with HBSS, cells were resuspended in 200 µl ice cold lysis buffer, containing 15 mM HEPES, pH 7.9, 200 mM KCl, 10 mM $MgCl_2$, 1% NP40, 10% glycerol, 20 µg/ml BSA, and 1 tablet Complete mini protease inhibitor EDTA free (Roche) per 10 ml buffer. Next, samples were sonicated 3 times 5 sec using ultrasound with amplitude 60 at 4°C. After 1 hour head-over-head incubation at 4°C, extracts were centrifuged for 15 min at 10,000 x g and 4°C and supernatant was isolated.

For brain homogenates, slices from frozen unfixed human brain tissue were collected using a sliding microtome (Leica SM 2010 R.). Tissue was homogenized using ceramic MagNA Lyser beads (Roche) by grinding in a Bullet Blender (Next Advance) for 3 min at strength 8 in lysis

buffer as described previously (Hu *et al.*, 2009). Homogenates were incubated for 1 hour in a head-over-head rotator at 4ºC, and centrifuged for 15 min at 10,000 x g at 4ºC.

Protein concentrations were determined with the bicinchoninic acid kit (BCA) (Thermo Fisher Scientific, Waltham, USA) using Bovine Serum Albumin (BSA) as a standard. After addition of 5% glycerol, samples were aliquotted, snap frozen and stored at -80°C.

Western blotting

SDS-PAGE separation of proteins was performed according to the "shorter CAG repeats" protocol as described previously (Hu *et al.*, 2009). Proteins were transferred to a 0.2 µm nitrocellulose membrane (Bio-Rad, #170-4159.) using the Trans-blot Turbo (BioRad) at 2.5A (constant)/25V for 10 min. Membranes were blocked for 15 min in tris buffered saline (TBS) containing 5% non-fat milk (Nutricia, Schiphol, the Netherlands). Next, membranes were incubated with primary rabbit antibody EPR5526 (Abcam, Cambridge, UK) that recognizes the N-terminus of the htt protein, diluted 1:5000 in blocking buffer, followed by secondary incubation with rabbit IRDye800 (LI-COR, Lincoln, USA) diluted 1:5000 in blocking buffer. Blots were analyzed on an Odyssey reader (LI-COR). Protein bands corresponding to wild-type and mutant htt were quantified using the Odyssey software version 3.0 (LI-COR). Background correction was performed by sampling an empty area of the blot of the same size as the area that contained the positive protein band. Wild-type and mutant htt protein expression levels relative to total htt protein expression were calculated by dividing wild-type and mutant htt band intensities with total htt band intensity (wild-type + mutant).

Dot blot assay

Brain homogenates were prepared in 150 mM sucrose, 15 mM HEPES pH 7.9, 60 mM KCl, 5 mM EDTA, 1 mM EGTA and 1 tablet Complete mini protease inhibitor EDTA free (Roche) per 10 ml buffer. Tissue was homogenized using ceramic MagNA Lyser beads (Roche) by grinding in a Bullet Blender (Next Advance) for 3 min at strength 8. Next, Triton X-100 (Sigma) was added to a final concentration of 1%. Homogenates were incubated in a head-over-head rotator for 1 hour at 4ºC and extracts were centrifuged for 10 min at 10,000 x g. Protein pellets were washed three times in 60 mM Tris and centrifuged for 10 min at 10,000 x g. Next, pellets were resuspended in 15% SDS and incubated overnight at 95ºC. Protein concentrations of the resulting pellet suspensions were determined by BCA. Per well, 100 µg of pellet suspension was applied to in 0.2% SDS pre-wetted cellulose acetate pore size 0.2 µm (Schleicher and Schuell, St. Louis, USA) membranes by vacuum application using the Bio-dot manifold (Bio-Rad). Wells were washed twice with 0.2% SDS and membrane was fixed in 0.5% glutaraldehyde for 20 min. The fixed membrane was blocked in TBS containing Tween-20 (TBST) and 5% non-fat milk (Nutricia). First incubation was performed with rabbit EPR5526 antibody diluted1:5,000 in TBST containing 5% non-fat milk. Secondary incubation was performed with mouse anti rabbit antibody conjugated with horse radish peroxidase (Santa Cruz, Dallas, USA), diluted 1:10,000 in TBST containing 5% non-fat milk. Membranes were incubated with enhanced chemiluminescence (ECL) (GE Healthcare, Cleveland, USA) and exposed to light sensitive film.

Statistical analyses

GraphPad Prism version 6.02 was used for statistical analysis. Typically, significance was determined using the two-tailed paired Student's t-test after testing for normal distribution. Data presented as bar graphs (means + standard deviation (SD)), whisker boxplots (whiskers = 10-90 percentile), or scatter dot plot (line = mean).

2.4. Results

No difference in wild-type and mutant HTT mRNA levels in HD patient-derived fibroblasts

To measure both wild-type and mutant HTT mRNA levels we performed a PCR with primers flanking the CAG repeat that separated on gel electrophoresis due to differences in their CAG repeat length (**Figure 1a**). In total four HD patient-derived fibroblasts of which 1, GM04857, contained a homozygous CAG repeat expansion were analyzed. For more information, see **Table 1**. Genomic DNA (gDNA) was taken along to control for differences in PCR amplification efficiencies across the CAG repeat. Furthermore, reverse transcription without reverse transcription enzyme was taken along, verifying that there was no gDNA contamination in our RT-PCR (**Figure 1b**). The two PCR products for each cell line were quantified and individual wild-type versus mutant HTT mRNA expression ratios were calculated. Next, the average expression levels of wild-type and mutant HTT mRNA in the adult-onset HD fibroblasts were calculated. No significant difference (P = 0.5168) between wild-type and mutant HTT mRNA expression was observed (**Figure 1c**).

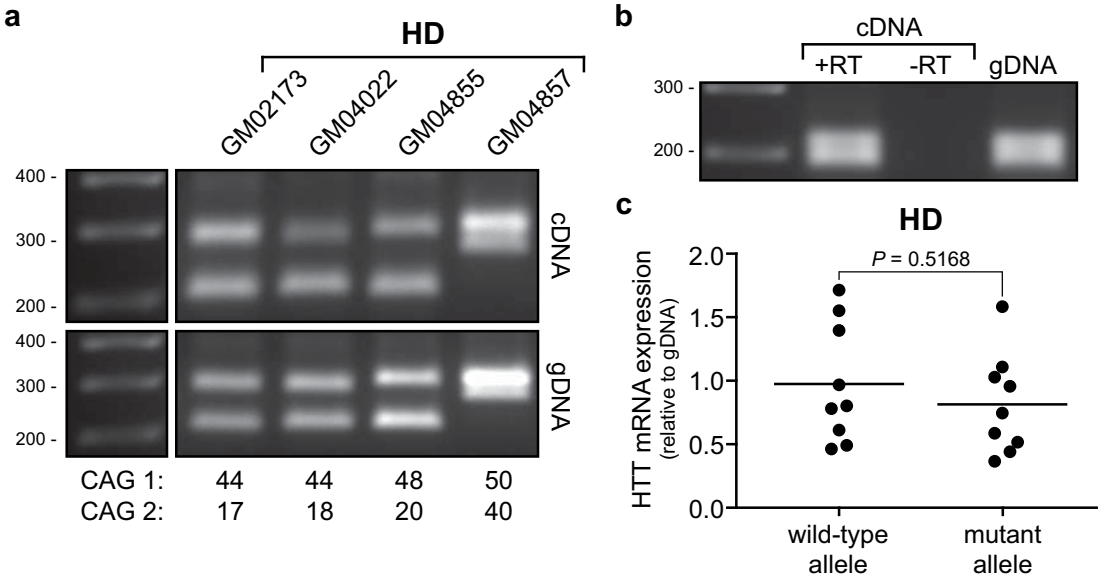

Figure 1. Wild-type and mutant HTT mRNA levels in HD patient-derived fibroblasts. Wild-type and mutant HTT mRNA PCR products were separated on gel electrophoresis by differences in their CAG repeat length. **(a)** RT-PCR products from 3 HD (GM02173, GM04022, GM04855) and one homozygous HD (GM04857) fibroblasts. Allelic CAG repeat sizes are indicated below each lane. gDNA was taken along to control for differences in PCR amplification efficiencies across the CAG repeat. **(b)** RT-PCR products with input: cDNA (+RT), cDNA lacking reverse transcriptase (-RT) and gDNA of 1 control (GM04204). **(c)** Scatter boxplot of RT-PCR from HD patient-derived fibroblasts, comparing wild-type and mutant HTT mRNA expression levels, relative to gDNA. Line = mean, data were evaluated using two-tailed student-t test, n = 3.

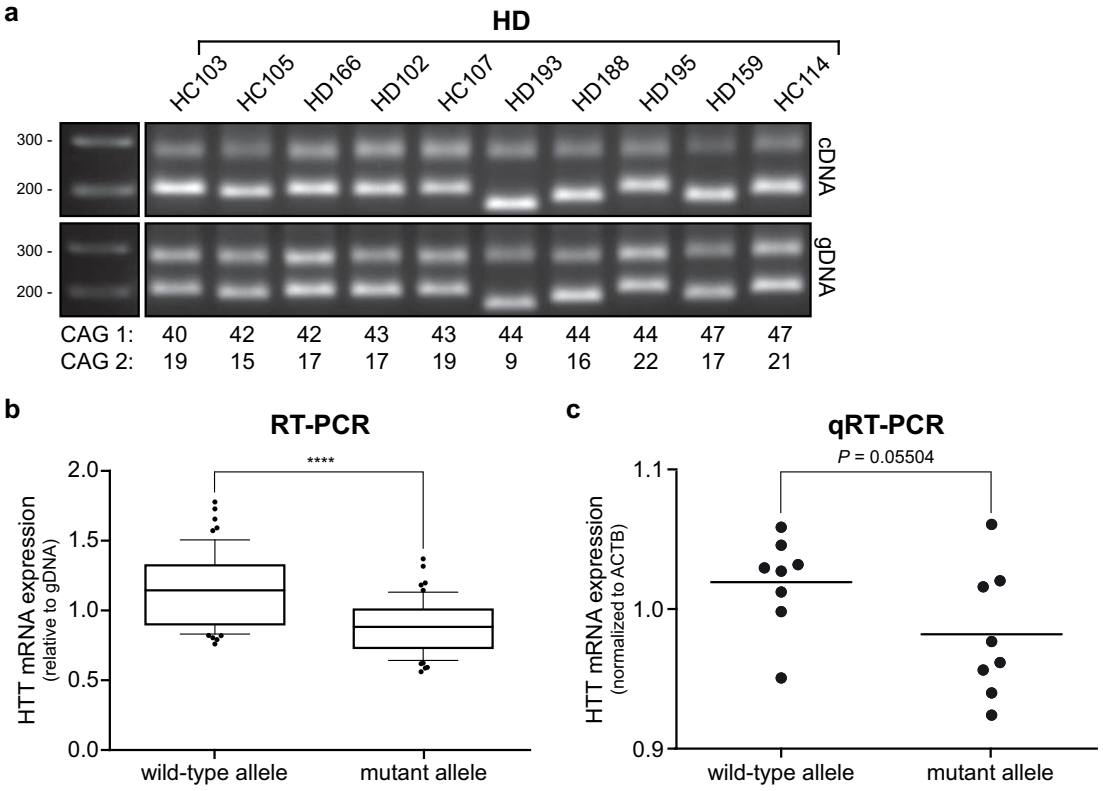

Figure 2. Wild-type and mutant HTT mRNA levels in HD human *post-mortem* brain material. Wild-type and mutant HTT mRNA PCR products were separated on gel electrophoresis by differences in their CAG repeat length. **(A)** RT-PCR products from brain tissue derived from 10 HD patients. Allelic CAG repeat sizes are indicated below each lane. gDNA was taken along to control for differences in PCR amplification efficiencies across the CAG repeat. **(B)** Whisker boxplot of HD RT-PCR data, comparing wild-type and mutant HTT mRNA expression levels, relative to gDNA. Whiskers = 10-90 percentile, data were evaluated using a two-tailed student t-test, **** $P < 0.0001$, n = 10. **(C)** Scatter boxplot of SNP rs362273-specific quantitative RT-PCR on HD *post-mortem* brain material, comparing wild-type and mutant HTT mRNA expression levels, normalized to β-actin (ACTB). Line = mean, data were evaluated using a two-tailed student t-test, n = 4.

More wild-type than mutant HTT mRNA in human *post-mortem* HD brain material

Next, we investigated HTT mRNA expression levels in *post-mortem* brain tissue from HD patients with a wide range of repeat lengths. RNA was isolated and PCR was performed with primers flanking the CAG repeat. PCR products were separated by gel electrophoresis due to differences in their CAG repeat length (**Figure 2a**). Individual bands were quantified and normalized against PCR products from gDNA (**Figure S1**).

After calculating average expression, wild-type and mutant HTT mRNA levels were compared (**Figure 2b**). Although the PCR approached the plateau phase, we still found a small, but significant, lower average mutant HTT mRNA expression 0.89 (±0.19) versus 1.15 (±0.25) of wild-type mRNA in *post-mortem* brain tissue from HD patients.

To validate the semi-quantitative RT-PCR gel electrophoresis analysis, we performed a SNP-

specific TaqMan quantitative PCR, using probes for SNP rs362273 located at exon 57 of HTT. Of our *post-mortem* brain samples, 6 out of 14 were heterozygous for SNP rs362273. Next, SNP linkage by circularization (SLiC) was successfully performed to determine which allele has the guanine and which allele the adenine in exon 57 (Liu *et al.*, 2008). Due to the variable RNA quality of brain tissue, SLiC was only possible in 4 out of 6 samples. The SNP-specific TaqMan quantitative (q)RT-PCR showed a consistent trend towards wild-type HTT. Due to the smaller number of brain samples that we could use for this SNP-specific TaqMan assay, the difference did not reach significance. However, it confirmed the higher expression of wild-type HTT mRNA compared to mutant HTT mRNA in HD *post-mortem* brain (**Figure 2c**).

No difference in wild-type and mutant htt protein levels in HD fibroblast and *post-mortem* brain

We examined levels of SDS-soluble wild-type and mutant htt protein levels in patient-derived fibroblasts by Western blot (**Figure 3a**). In the homozygous HD fibroblast GM04857, only one protein band was visible because the difference in protein size between the htt protein expressed from the two alleles is too small to separate by Western blot. For the other samples, the separated wild-type and mutant htt protein bands were quantified and individual wild-type versus mutant htt protein ratios were calculated (**Figure S2**). Next, we averaged all data from individual measurements and compared wild-type and mutant htt protein levels. No significant difference between wild-type and mutant htt protein levels in patient-derived fibroblasts was found (**Figure 3c**).

We then analyzed SDS-soluble wild-type and mutant htt protein levels in *post-mortem* human HD brain homogenates (**Figure 3b**). As with the HD fibroblasts, there was no difference in wild-type and mutant htt levels in HD brains (**Figure 3d** and **Figure S2**). We also examined aggregation of mutant htt in our *post-mortem* human HD brain tissue by investigating SDS-insoluble htt using a dot blot assay. We found comparable levels of SDS-insoluble htt for subjects HC105 and HD166, which had the same polyQ stretch of 44, and more insoluble htt for subject HC107 which had a slightly longer polyQ stretch of 45 (**Figure 3e**).

Soluble wild-type and mutant htt protein levels are similar in both fibroblasts and brain, while in fibroblasts it is known that mutant htt protein does not aggregate (Sathasivam *et al.*, 2001). We found more htt protein aggregation in the brain sample with the longer polyQ repeat, but there was no decrease in mutant htt protein levels on Western blot.

More wild-type than mutant htt protein in juvenile HD fibroblasts and *post-mortem* brain

Next, we used Western blot to analyze SDS-soluble levels of wild-type and mutant htt protein in juvenile HD samples. Analysis of juvenile HD fibroblast cell lines showed a significant higher level of wild-type htt protein compared to mutant htt (0.55 versus 0.45 (±0.05)) (**Figure 4a and c**). Western blot analysis of *post-mortem* juvenile HD brain lysates also showed a significantly higher level of wild-type htt protein with respect to mutant htt (0.53 versus 0.47 (± 0.06)) (**Figure 4b and d**).

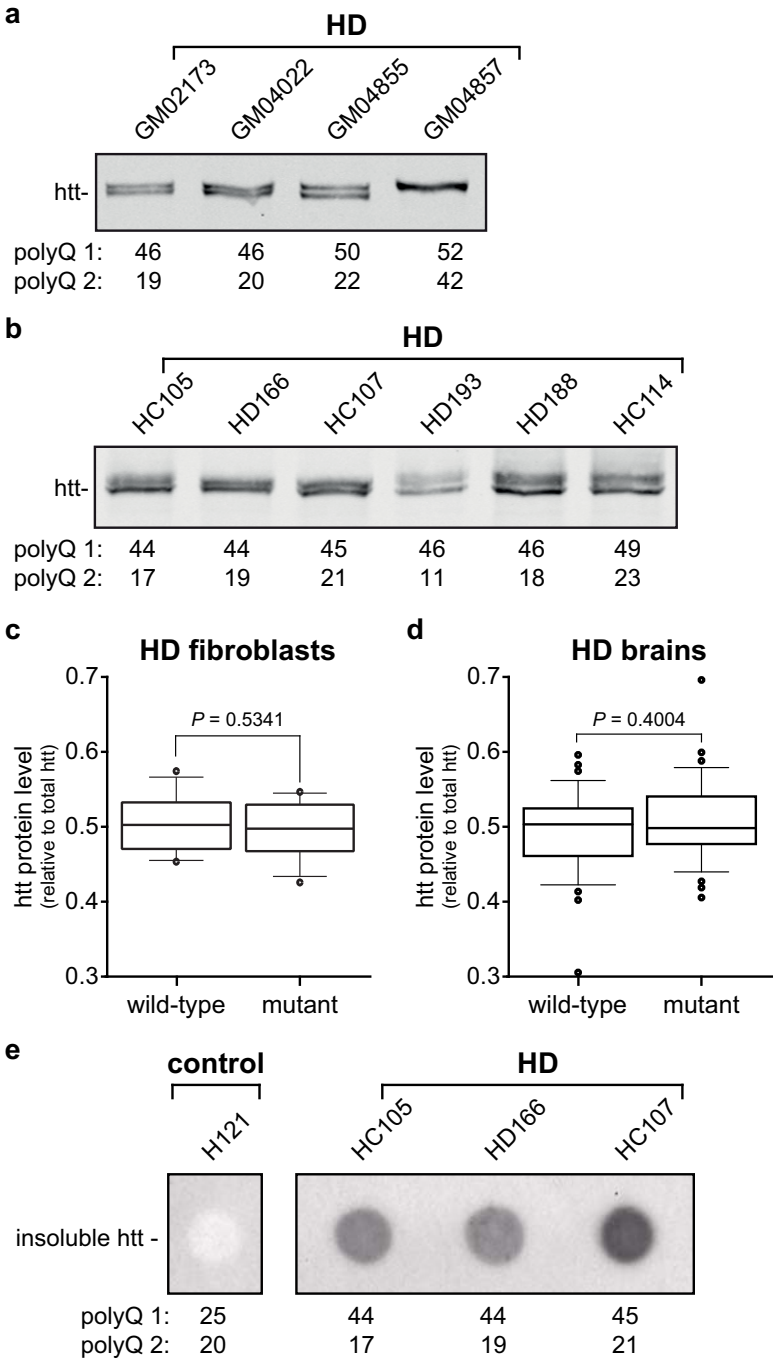

Figure 3. Wild-type and mutant htt protein levels in HD fibroblasts and *post-mortem* brain tissue. PolyQ repeat lengths are indicated below each lane. The lower band represents wild-type htt protein, the upper band mutant htt protein. **(a)** Western blot analysis of total protein lysates from human fibroblasts from three heterozygous HD (GM02173, GM04022, GM04855) and one homozygous HD subject (GM04857). **(b)** Western blot analysis of cortical brain homogenates from six HD subjects. **(c)** Whisker box plots comparing wild-type and mutant htt levels normalized against total htt in HD fibroblasts (n = 3) and **(d)** HD *post-mortem* brain tissue (n = 6). Whiskers = 10-90 percentile, data were evaluated using a two-tailed student t-test. **(e)** Dot blot assay of SDS-insoluble htt protein fractions of human control (H121) and HD brain (HC105, HD166, HC107). Dot intensity indicates level of insoluble htt protein.

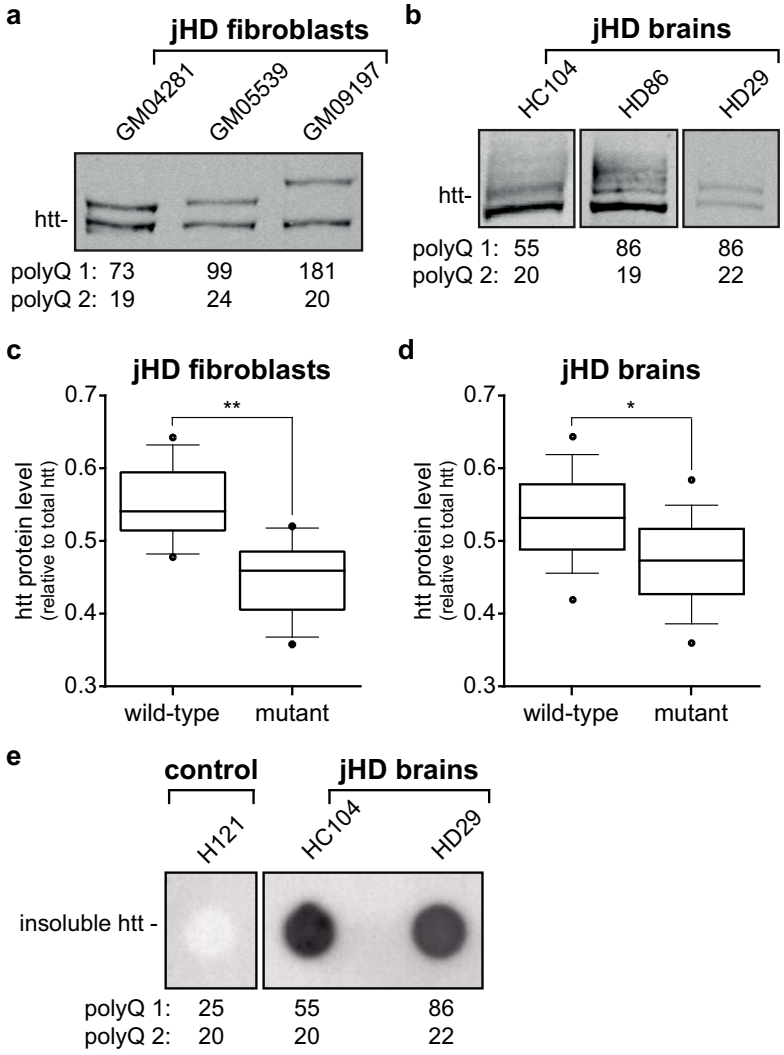

Figure 4. Wild-type and mutant htt protein levels in patient-derived juvenile HD fibroblasts and *post-mortem* brain tissue. (a) Western blot analysis of total protein lysates from human fibroblasts derived from three juvenile HD subjects. PolyQ repeat lengths are indicated below each lane. **(b)** *Post-mortem* cortical brain tissue from three juvenile HD subjects (GM04281, GM05539, GM09197). The lower band represents wild-type htt, the upper band mutant htt. **(c)** Whisker box plots comparing wild-type and mutant htt levels normalized against total htt in juvenile HD fibroblasts and **(d)** juvenile HD *post-mortem* brain tissue. Whiskers = 10-90 percentile, data were evaluated using a two-tailed student t-test, n = 3, * $P > 0.05$, ** $P > 0.01$. **(e)** Dot blot assay of SDS-insoluble htt protein fractions of human control (H121) and juvenile HD brain homogenates (HC104 and HD29). Dot intensity indicates level of insoluble htt protein. PolyQ repeat lengths are indicated below each lane.

We also looked at aggregation of *post-mortem* juvenile HD brain lysates from subjects HC104 and HD29 using the dot blot assay (**Figure 4e**). As expected, when compared with the HD brain lysates, juvenile HD brain lysates clearly showed more aggregated SDS-insoluble mutant htt protein.

To conclude, in adult-onset HD samples, wild-type and mutant htt protein levels are equal, regardless of mutant htt protein aggregation. In juvenile HD there is a consistent lower level of mutant htt protein expression, in both brain and fibroblast samples.

Identification of novel HTT antisense isoform in patient-derived fibroblasts and brain tissue

In previous studies in *post-mortem* HD brain it was suggested that the HTTAS_v1 with an expanded CTG repeat was not expressed (Chung *et al.*, 2011). To validate this a homozygous HD patient-derived fibroblast GM04857 was included since it has two expanded CAG repeats and therefore should not have any HTTAS_v1 expression. Unexpectedly, we also found HTTAS_v1 in fibroblasts obtained from an HD patient homozygous for the CAG repeat expansion (**Figure 5a**). The HTTAS_v1 expression level of the homozygous HD patient was comparable to that of the heterozygous patient samples, suggesting that there is expression of HTTAS_v1 with the expanded CTG repeat.

Next, we designed HTTAS isoform-specific primers to examine the expression of HTTAS_v1 and v2 in: (I) fibroblasts derived from a control, (II) an HD patient, and (III) a juvenile HD patient (**Figure 5a**), as well as *post-mortem* (juvenile) HD brain tissue (**Figure 5b**). Similar levels of HTTAS_v1 in all brain and fibroblasts samples were shown. Interestingly, the primers specific for HTTAS_v2 gave an additional band, slightly bigger than the expected PCR amplicon. Sanger sequencing confirmed that this was a novel HTTAS isoform, which we named HTTAS_v2.2 (**Figure 5c**). This HTTAS_v2.2 has an additional 69 nucleotides at the 3'end of HTTAS exon 2.

In sum, similar HTTAS expression levels in (homozygous) HD and controls were found, suggesting that the observed variations in wild-type and control HTT transcript levels in *post-mortem* brain are probably not caused by changes in HTTAS expression levels. Furthermore, we have identified a novel HTTAS isoform, which we named HTTAS_v2.2.

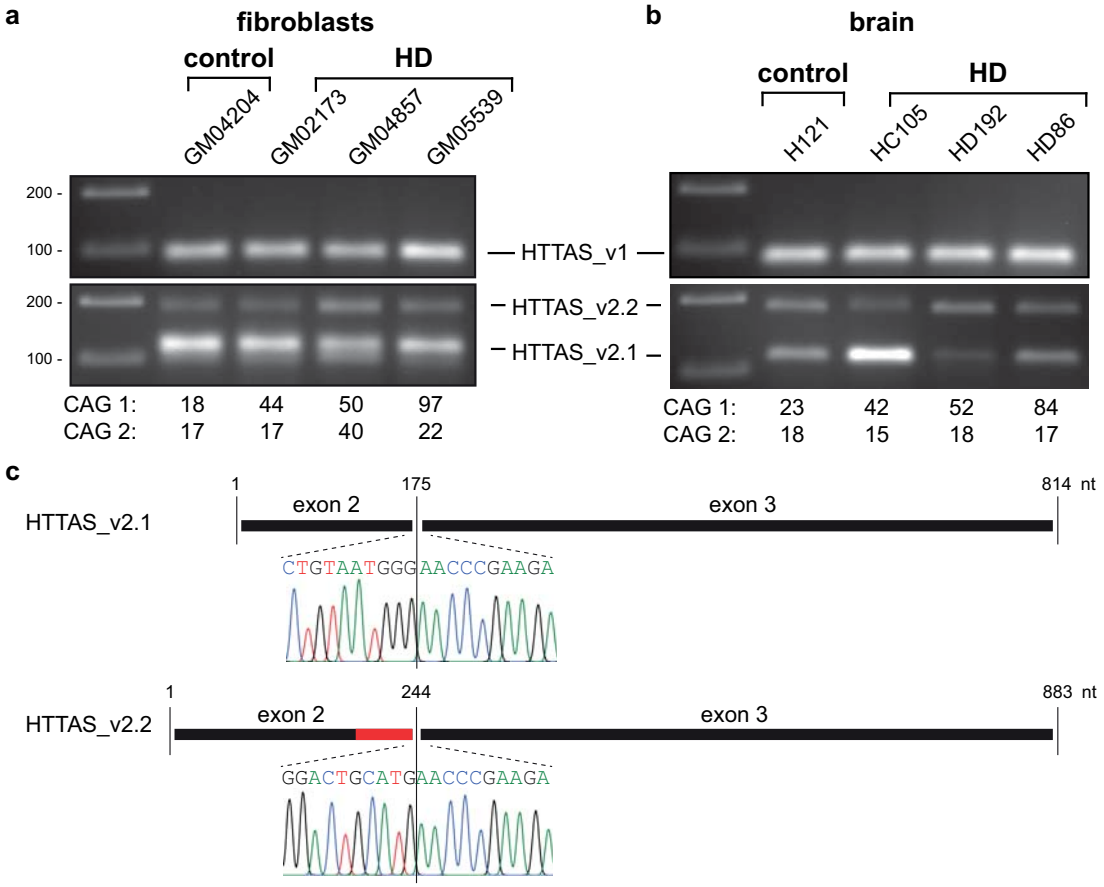

Figure 5. HTT antisense (HTTAS) identification in HD patient-derived fibroblasts and *post-mortem* brain tissue. HTTAS_v1 and HTTAS_v2 were amplified using strand- and HTTAS isoform-specific primers. **(a)** Gel electrophoresis of HTTAS_v1 and HTTAS_v2 RT-PCR of patient-derived fibroblasts from a control (GM04204), an HD patient (GM02173), an HD patient homozygous for the CAG repeat expansion (GM04857) and a juvenile HD patient (GM05539). **(b)** Gel electrophoresis of HTTAS_v1 and HTTAS_v2 RT-PCR of *post-mortem* brain tissue from a control (H121), an HD patient (HC105), and 2 juvenile HD patients (HD192 and HD86). Allelic CAG repeat sizes below each lane. **(c)** Schematic representation of HTTAS_v2.1 and the novel identified HTTAS_v2.2. Sanger sequencing of the exon 2 - exon 3 boundaries of both HTTAS_v2 isoforms are shown. The novel HTTAS_v2.2 has an additional 69 nucleotides at the 3'end of HTTAS exon 2.

2.5. Discussion

In the current study we found that in adult-onset HD patient-derived fibroblasts, the levels of wild-type and mutant HTT mRNA did not significantly differ. This is in concordance with results found in patient-derived HD lymphoblasts (Lee *et al.*, 2013). By analyzing microarray probes that detect both wild-type and mutant HTT mRNA, it was shown that the expanded CAG repeat did not affect HTT mRNA expression (Lee *et al.*, 2013). CAG repeat-induced RNA toxicity has recently also been proposed to be involved in the HD pathogenesis (Wojciechowska and Krzyzosiak, 2011). The size of the CAG repeat is thought to be critical for the contribution of RNA toxicity (Wang *et al.*, 2011). Juvenile fibroblast cells with mutant htt alleles containing either 68 or 151 CAGs exhibited aggregation of mutant HTT mRNA (de Mezer *et al.*, 2011). Our results show that there is no difference in wild-type and mutant HTT mRNA levels in fibroblasts, suggesting that there is no detectable effect of mRNA aggregation on mRNA levels in adult-onset fibroblast samples. However, in *post-mortem* brain tissue we did find a small but significant lower level of mutant than wild-type HTT mRNA, highlighting subtle differences between *post-mortem* brain tissue and patient-derived fibroblasts.

Wild-type and mutant htt protein levels did not significantly differ in either patient-derived fibroblasts or *post-mortem* brain samples. Soluble htt has a half-life of approximately 24 hours (Persichetti *et al.*, 1996) and we hypothesize that with Western blot analysis we detect soluble htt that is present in the cells. Aggregated htt is less efficiently cleared (Gutekunst *et al.*, 1999). This SDS-insoluble accumulated htt protein is detected by dot blot assay. Since protein aggregation is an important feature in HD brain tissue, but does not occur in HD fibroblasts (Sathasivam *et al.*, 2001), our results show that protein aggregation does not affect the levels of soluble htt protein. Although htt protein levels did not differ, in human brain samples we did find less mutant HTT mRNA. A possible explanation could be an enhanced translation of mutant HTT, resulting in equal htt protein levels. Recently, increased translation of mutant htt by binding of the MID1-PP2A translational complex was shown (Krauss *et al.*, 2013). Cells overexpressing N-terminal htt fragments with a normal and mutant polyQ repeat showed an enhanced protein synthesis of htt fragments with an expanded polyQ repeat. This more efficient translation of mutant HTT mRNA was proposed to be caused by enhanced binding of the MID1-complex to the expanded CAG repeat and mediated by mTOR and S6K kinases (Krauss *et al.*, 2013). However, this cannot be a general expanded polyQ mechanism, since we only found a difference in wild-type and mutant HTT mRNA in brain tissue samples and not in fibroblast cells. Another possible explanation for the differences in HTT mRNA levels between human fibroblasts and brain could be the nature of the tissue where RNA was isolated from; dividing living cells versus brain material with *post-mortem* delay and subsequently autolysis. Nevertheless, our results show subtle differences in htt protein levels between *post-mortem* brain tissue and patient-derived fibroblasts. This has to be considered when interpreting results obtained from patient-derived HD fibroblasts or other peripheral tissue with respect to disease processes in HD.

In juvenile HD samples we consistently found that the levels of wild-type htt protein were higher than mutant htt protein in both patient-derived fibroblasts and *post-mortem* brain tissue. This is in contradiction with previous studies in knock-in HD mice carrying one or two repeats with 111 CAGs (Krauss *et al.*, 2013), which showed increased mutant htt protein levels. It is known that reverse transcriptase and polymerase chain reactions across CG-rich regions are notoriously difficult (Stine *et al.*, 1995), this combined with a reduced RNA quality in our juvenile HD samples, is why we could not reliably quantify mutant HTT mRNA levels in juvenile HD subjects. It is conceivable that the lower mutant htt protein level in juvenile HD is caused by an equivalent lower level of mutant HTT mRNA. Clearly, our results indicate that expression of wild-type and mutant htt in juvenile HD are different compared to that of adult-onset HD.

Recently it has been suggested that in polyQ disorders bidirectional RNA transcription could play a role in the disease pathology by deregulation of the sense transcript (Chung *et al.*, 2011; Sopher *et al.*, 2011). In HD, two natural HTTAS transcripts (HTTAS_v1 and v2) were identified at the HTT locus, of which HTTAS_v1 contained the CTG repeat (Chung *et al.*, 2011). It was shown that overexpression of HTTAS_v1with an wild-type repeat resulted in reduced HTT sense transcript levels, whereas knockdown of HTTAS_v1 increased HTT sense transcript levels. Based on these findings, it was hypothesized that HTTAS_v1 negatively regulated htt transcript expression (Chung *et al.*, 2011). Also, when the CTG repeat in HTTAS_v1 was expanded, expression was strongly reduced in HD brains. However, our results show expression of HTTAS_v1 in human-derived fibroblasts homozygous for the CAG repeat expansion, suggesting that there is an HTTAS_v1 with expanded CTG repeat transcribed. Unfortunately we did not have *post-mortem* material from a homozygous HD patient to validate this HTTAS_v1 expression in human homozygous HD brain. Furthermore, we have identified a novel HTTAS_v2 isoform, which has an additional 69 nucleotides at the 3'end of HTTAS exon 2, which we named HTTAS_v2.2. Future research will have to determine the role of these antisense transcripts in HTT expression.

Recent advances have shown the potential of reducing mutant htt levels with oligonucleotide-based therapeutics. Reduction of both wild-type and mutant htt up to 70% was well tolerated in HD rodent models and non-human primates (Kordasiewicz *et al.*, 2012). Long-term suppression of wild-type and mutant htt might not be desirable because of htt's anti-apoptotic function (Rigamonti *et al.*, 2000) and importance for cell survival in the adult brain (Dragatsis *et al.*, 2000; Zhang *et al.*, 2003). A different approach would be an allele-specific reduction of mutant htt. This could be achieved with oligonucleotides directed against SNPs unique to the mutant htt transcript, or by targeting the expanded CAG repeat directly (Appl *et al.*, 2012). Showing that the basal levels of mutant HTT mRNA and mutant htt protein are equal or lower when compared to wild-type, provides feasibility for oligonucleotide therapeutics that are not completely specific for the mutant HTT allele.

Our results highlight subtle differences in htt RNA and protein expression with less mutant HTT mRNA, but equal wild-type and mutant htt protein levels in adult-onset HD. In juvenile HD mutant htt protein levels were lower compared with wild-type htt, indicating subtle differences in htt protein expression between adult-onset and juvenile HD. Differences between *post-mortem* brain tissue and patient-derived fibroblasts have to be taken into account when

interpreting results obtained from HD patient-derived fibroblasts. Furthermore, differences in htt levels between adult-onset HD and juvenile HD samples should be taken into account when using HD tissue and animal models with juvenile polyQ repeat lengths.

2.6. Acknowledgements

We thank David F. Fischer (BioFocus, a Galapagos company, Leiden, The Netherlands) and Michela A. Tessari (Galapagos B.V., Leiden, The Netherlands) for the TaqMan SNP assay. We thank Marika Eszes and Ingrid Hegeman for providing us with the relevant clinical information.

This work was supported by the Center for Biomedical Genetics (the Netherlands), the Prinses Beatrix Spierfonds (the Netherlands), and Integrated European Project in Omics Research of Rare Neuromuscular and Neurodegenerative Diseases (Neuromics). The funders had no role in study design, data collection and analysis, decision to publish, or preparation of the manuscript.

2.7. Supplementary Material

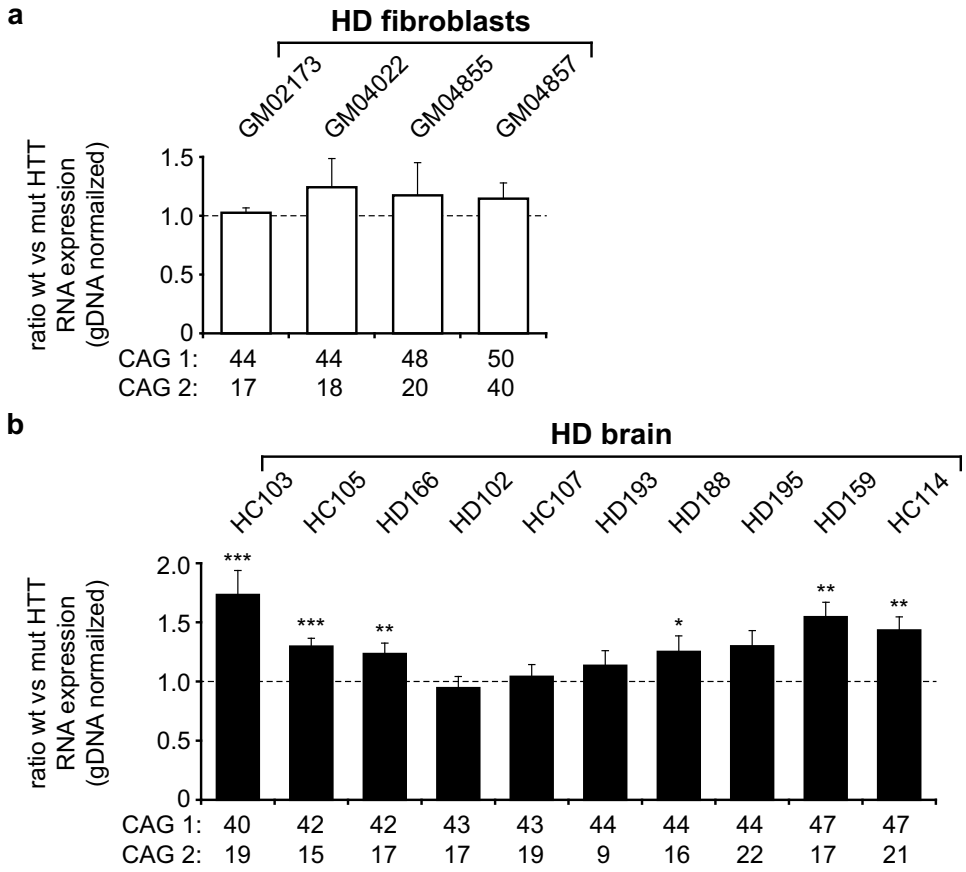

Figure S1. Wild-type and mutant HTT mRNA levels in individual HD patient-derived fibroblasts and post-mortem brain material. Wild-type and mutant HTT alleles were separated by differences in CAG repeat length. Allelic CAG repeat sizes below each bar. gDNA was taken along to control for the PCR reaction over the CAG repeat. Wild-type and mutant HTT RNA expression levels were calculated by dividing the intensity of the gDNA normalized wild-type HTT band by the mutant HTT band. **(a)** Gel electrophoresis quantification of 4 HD fibroblasts. Bars represent mean values with standard deviation (n = 3). **(b)** Gel electrophoresis quantification of brain tissue derived from 10 HD patients. Bars represent mean values with standard deviation. Data were evaluated using two-tailed student-t test, * $P > 0.05$, ** $P > 0.01$, *** $P > 0.001$, n = 5.

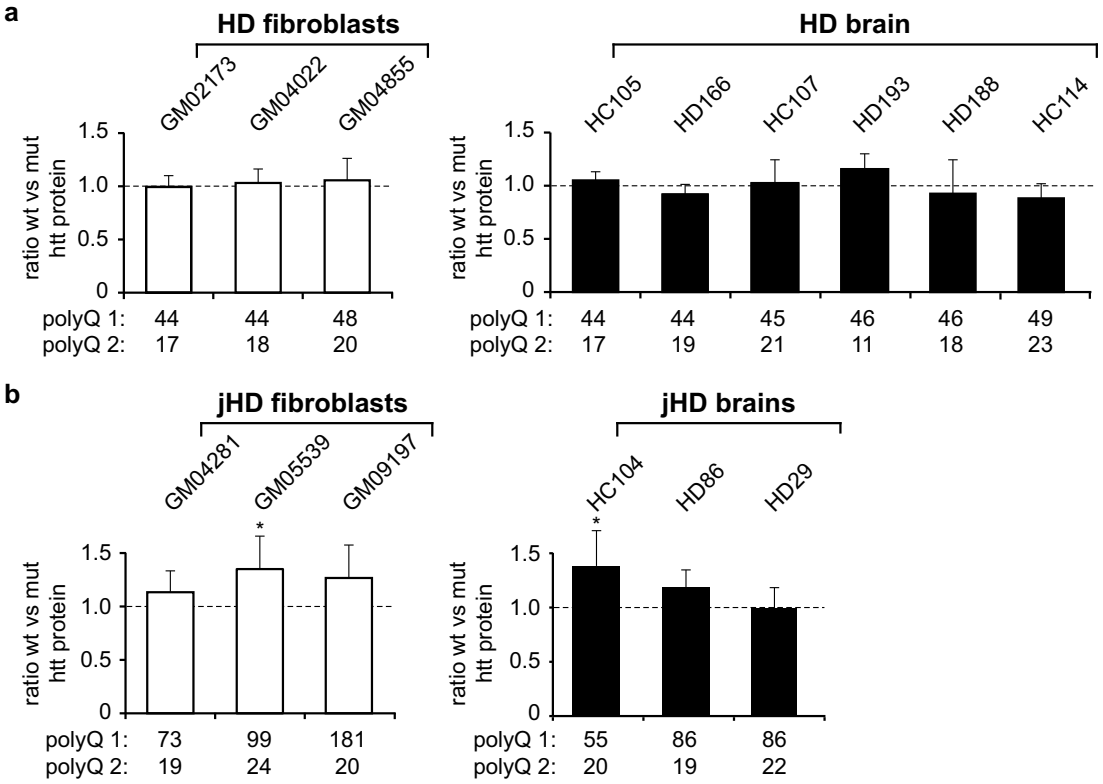

Figure S2. Analysis of wild-type and mutant htt ratio's in individual subjects. Wild-type versus mutant htt ratio for individual subjects was calculated by dividing wild-type htt band intensity with mutant htt band intensity. Individual polyQ tracts are indicated below each subject. **(a)** Individual patient-derived HD fibroblast cell lines (left), or individual post-mortem cortical brain lysates (right). **(b)** Individual patient-derived juvenile HD fibroblast cell lines (left), or individual post-mortem cortical juvenile HD brain lysates (right). Bars represent mean values with standard deviation (n ≥ 3). Data were evaluated using two-tailed student-t test, * $P < 0.05$.